Lanthanide luminescent di-metallic triple-stranded helicates formed from bis-tridentate (1,2,3-triazol-4-yl)-picolinamide (tzpa) ligands and their higher order self-assemblies

Dawn E. Barry,[a] Oxana Kotova,[a,b] Niamh A. O'Shea,[a,b] Shauna R. Donohoe,[a] Aramballi J. Savyasachi,[a,b] and Thorfinnur Gunnlaugsson*[a,b]

[a]*School of Chemistry and Trinity Biomedical Sciences Institute (TBSI), Trinity College Dublin, The University of Dublin, Dublin 2, Ireland. E-mail: gunnlaut@tcd.ie*
[b]*Advanced Materials and BioEngineering Research (AMBER) Centre, Trinity College Dublin, The University of Dublin, Dublin 2, Ireland*

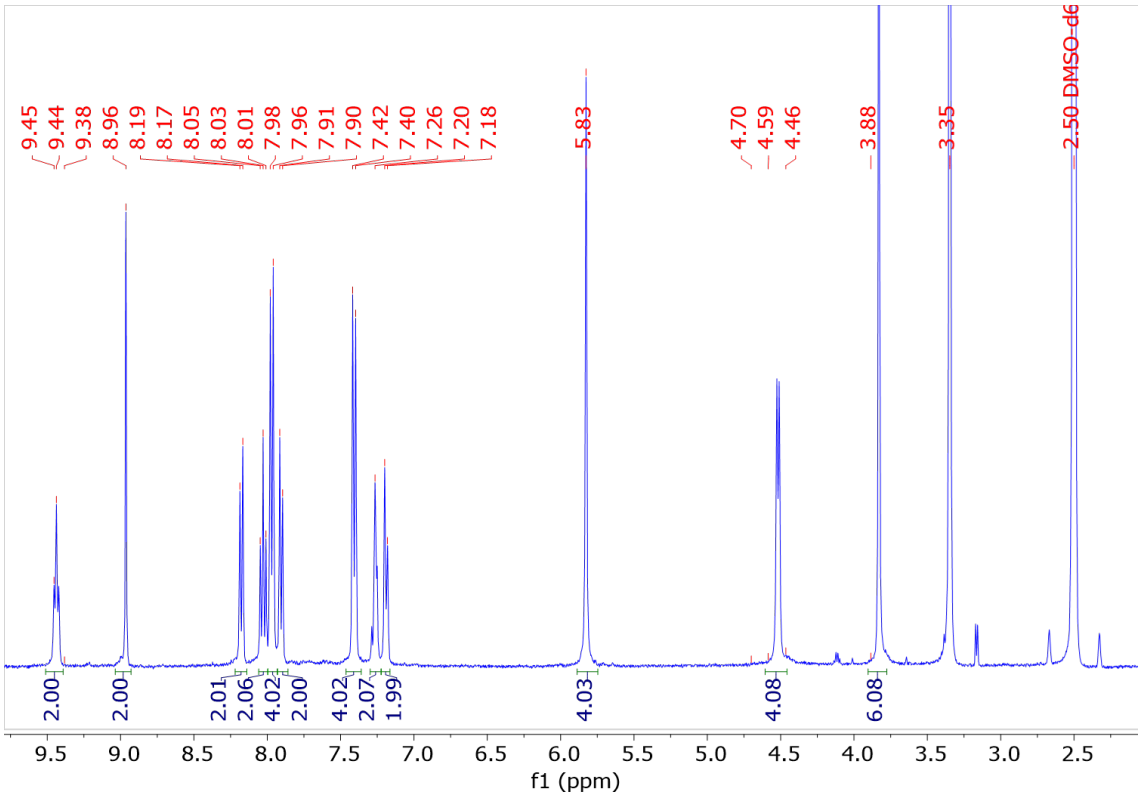

Figure S1. ^{1}H NMR of **1** (DMSO-d6, 400 MHz).

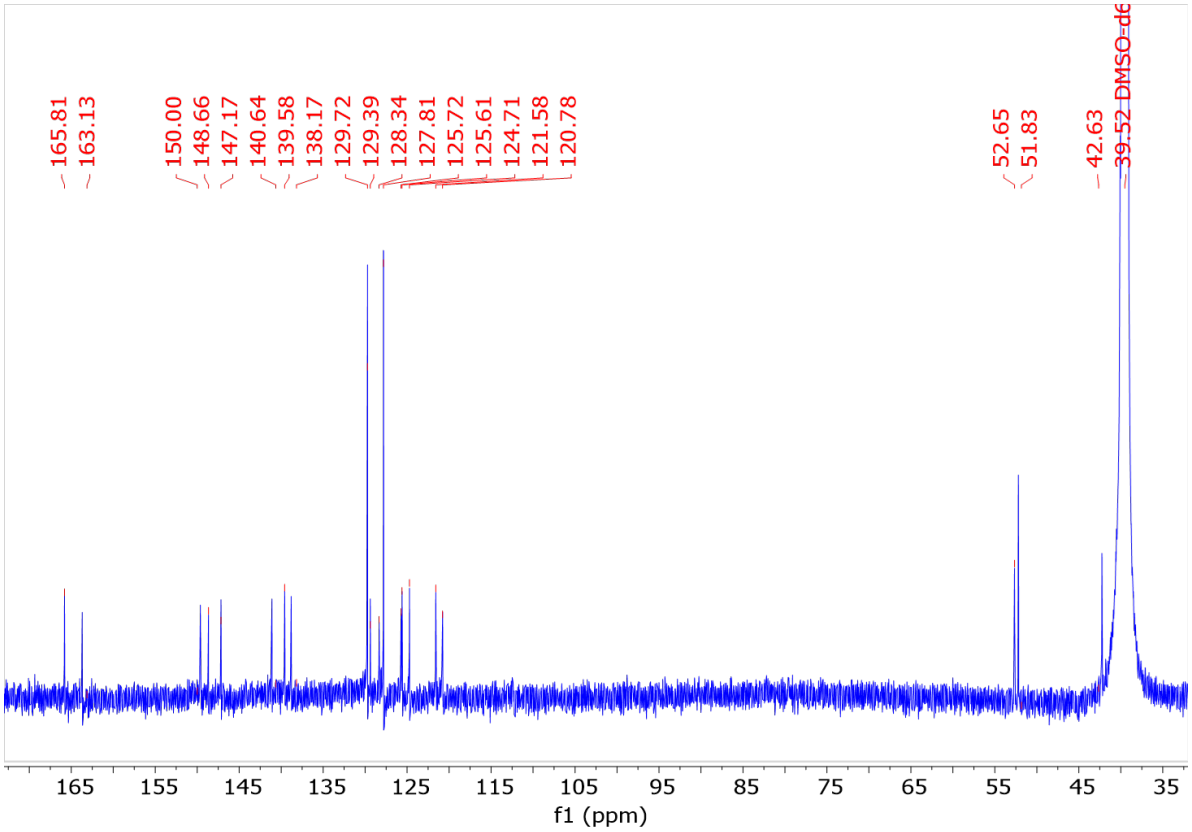

Figure S2. ^{13}C NMR of **1** (DMSO-d6, 400 MHz).

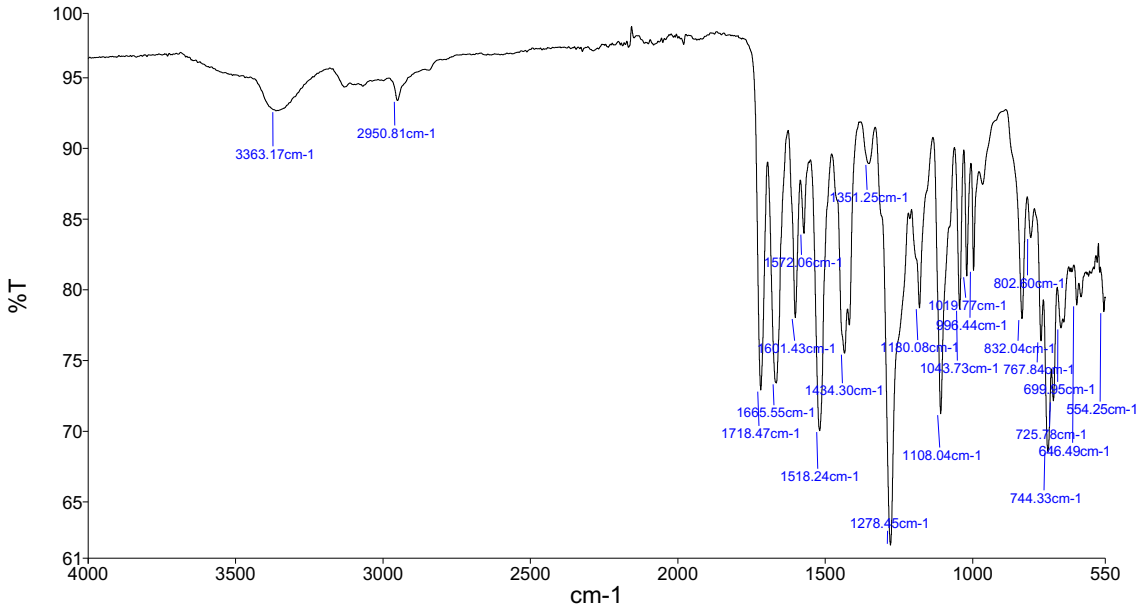

Figure S3. IR spectrum of **1**.

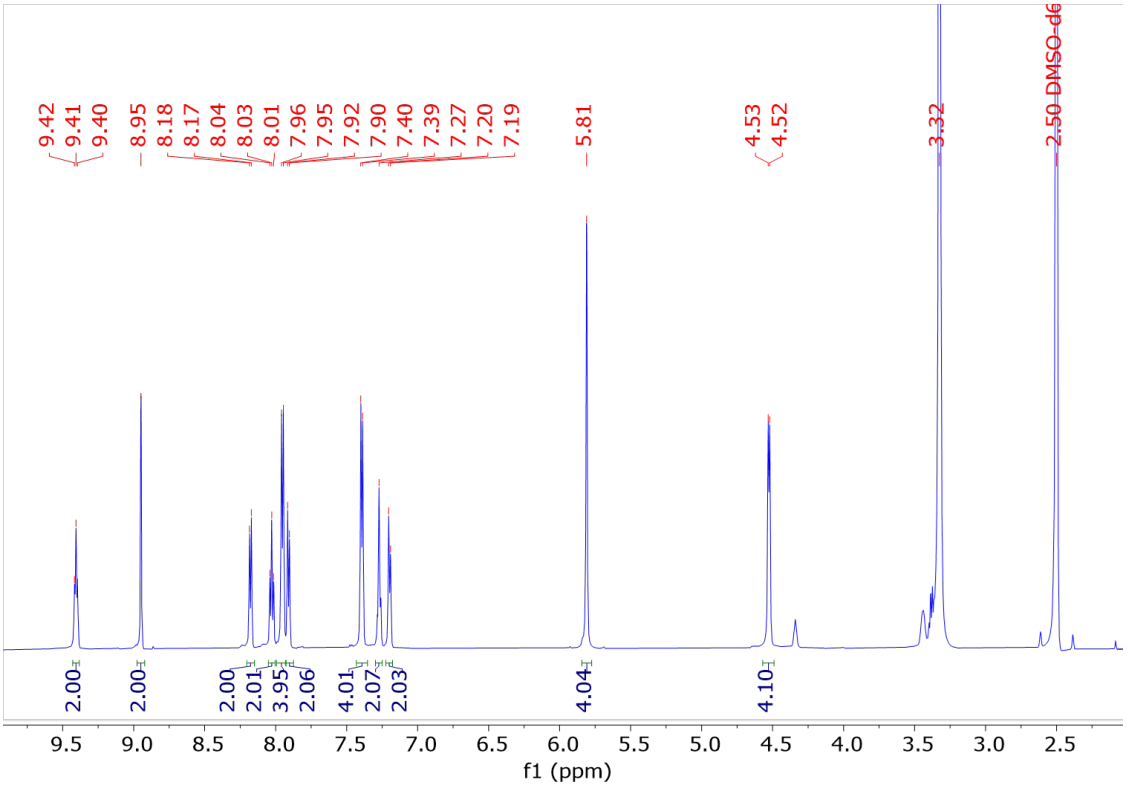

Figure S4. ^{1}H NMR of **1a** (DMSO-d6, 600 MHz).

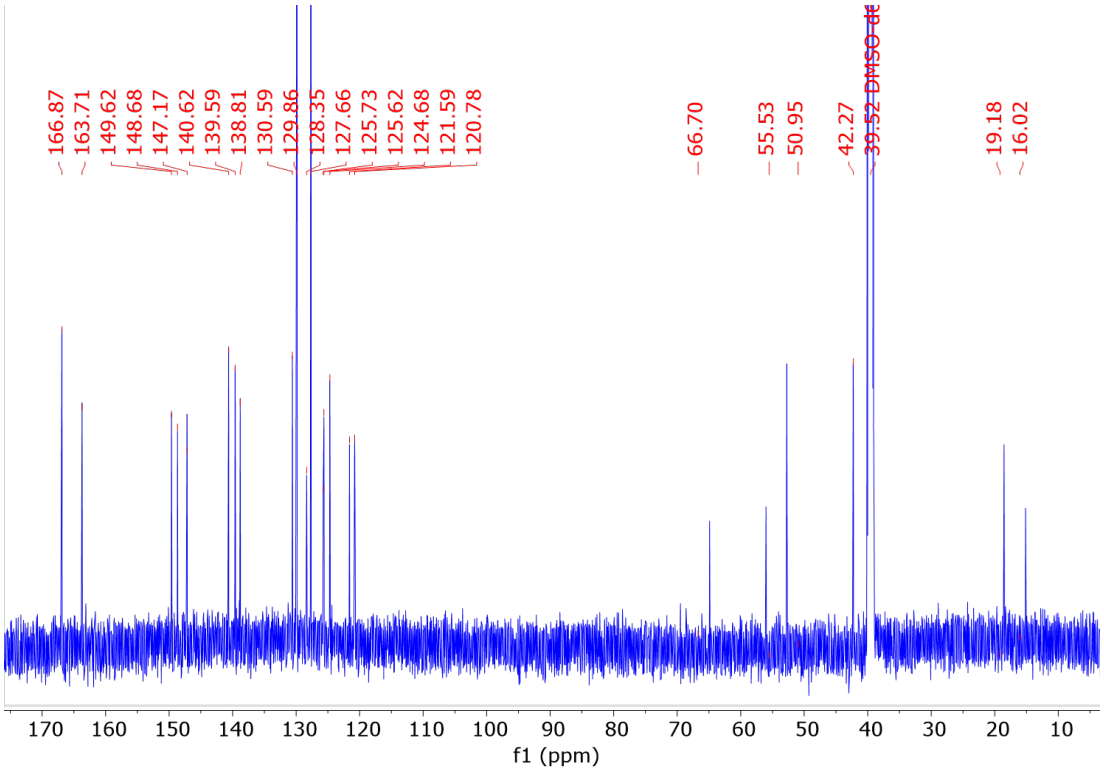

Figure S5. ^{13}C NMR of **1a** (DMSO-d6, 150 MHz).

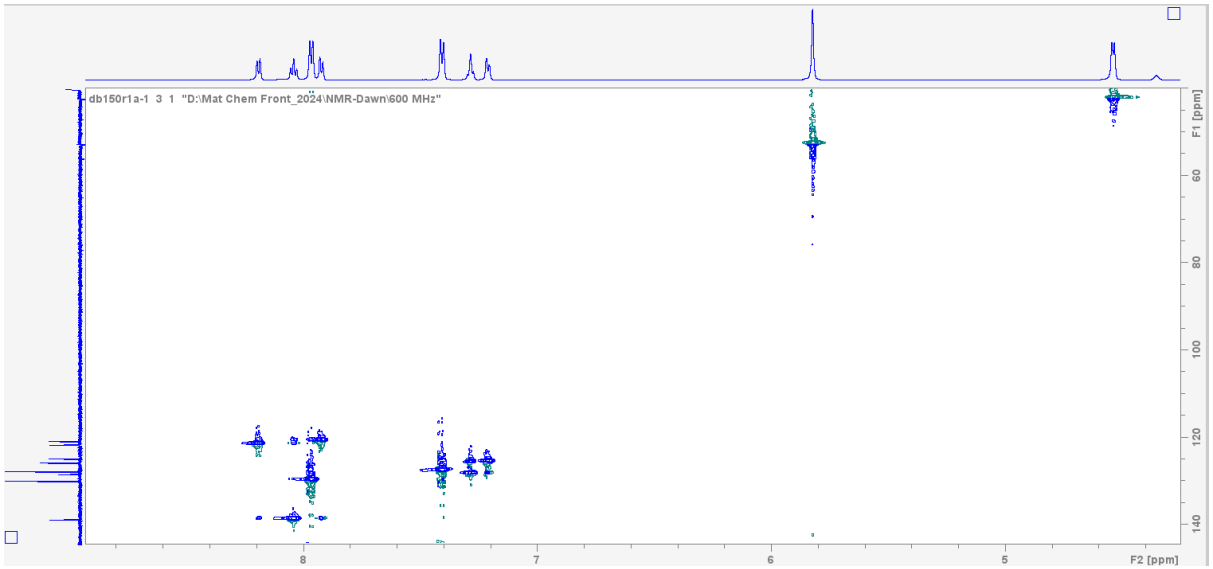

Figure S6. HSQC of **1a** (DMSO-d_6).

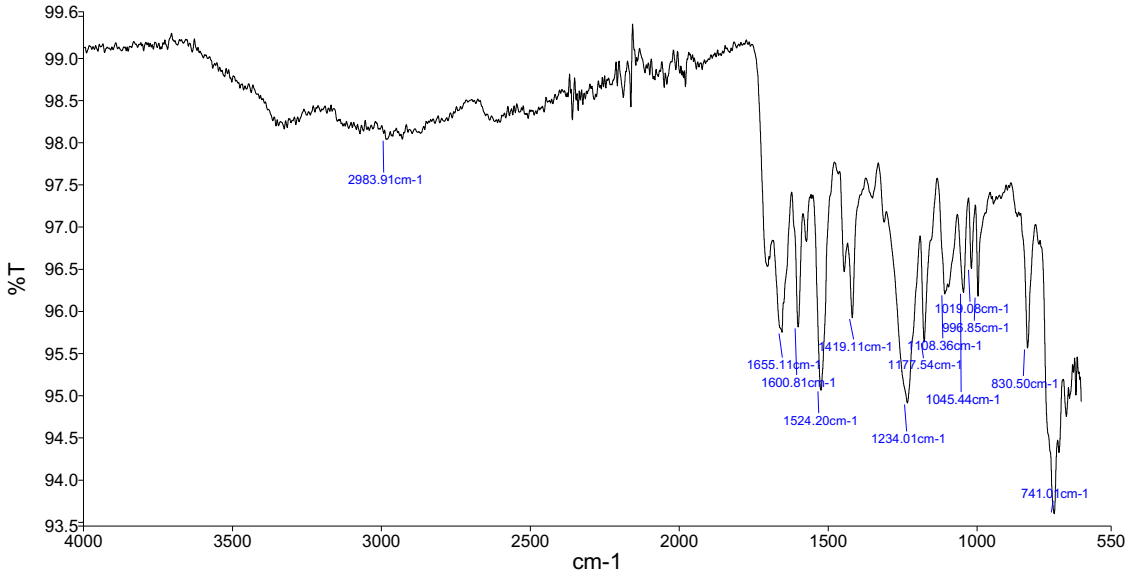

Figure S7. IR of **1a**.

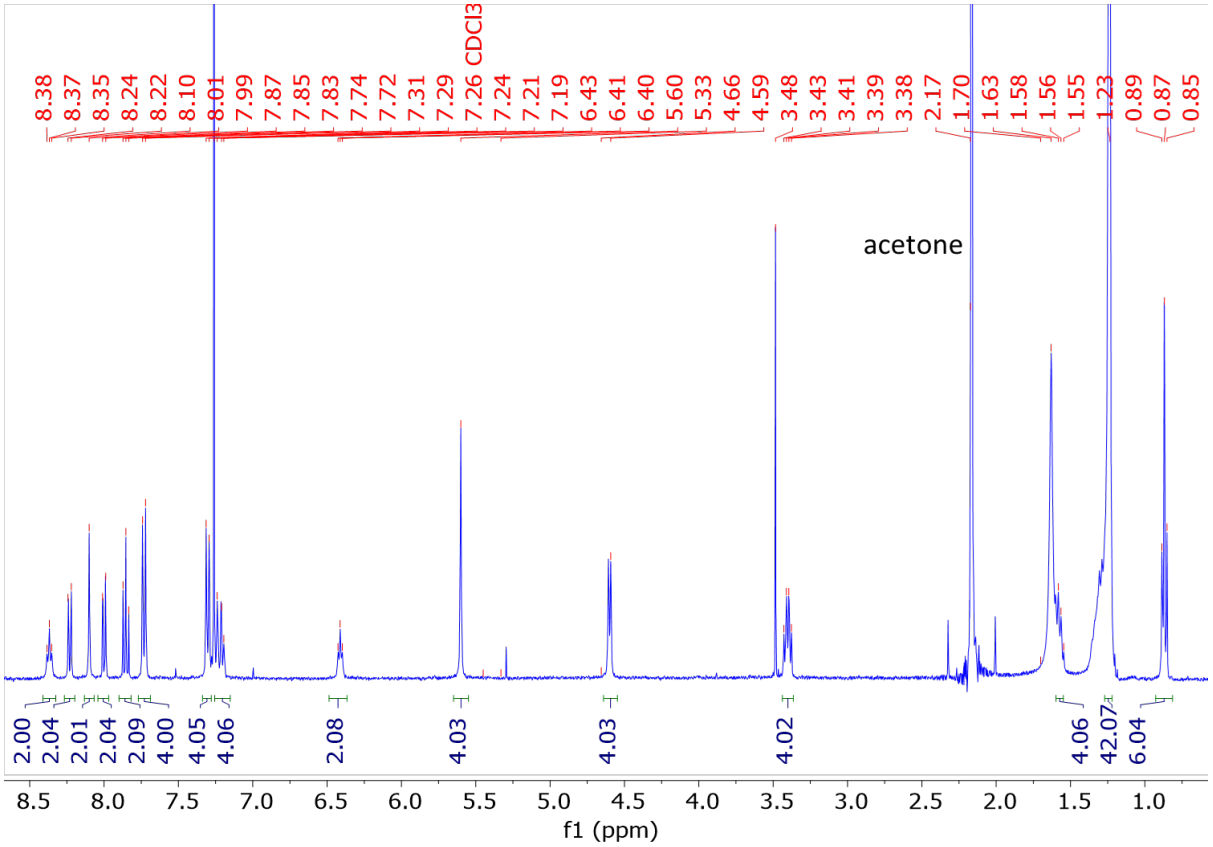

Figure S8. ^{1}H NMR of **2** ($CDCl_3$, 400 MHz).

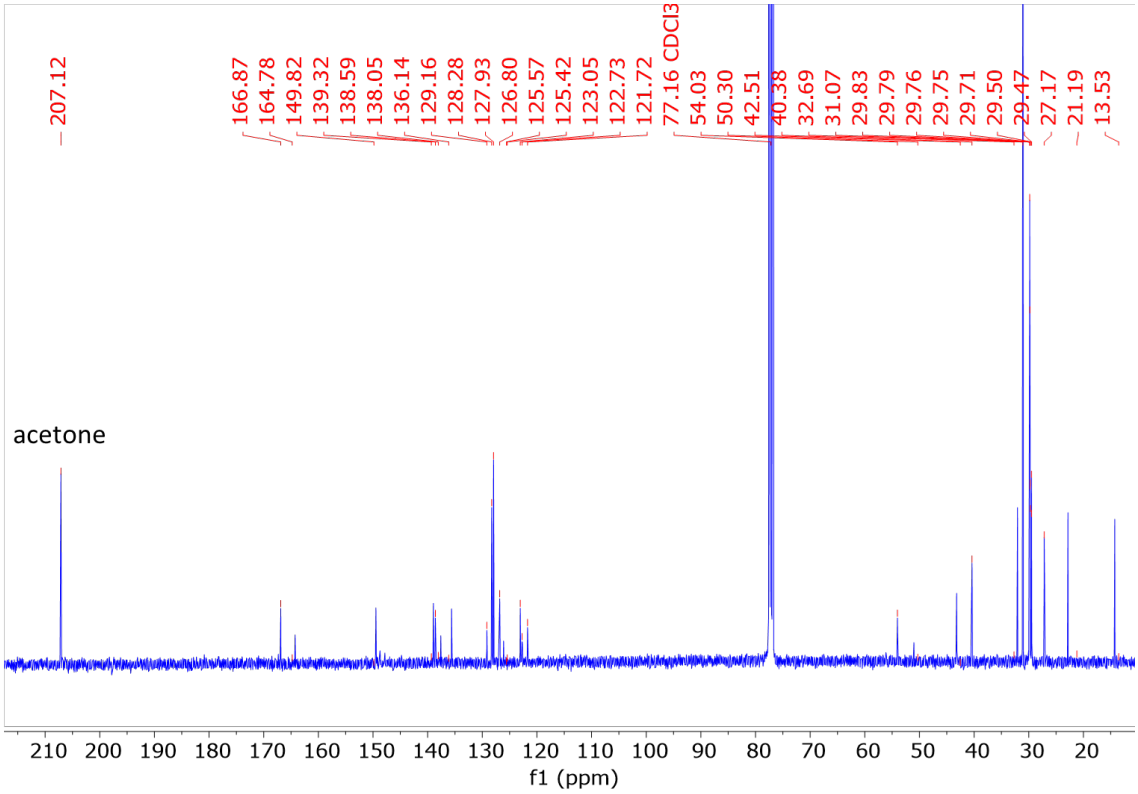

Figure S9. ^{13}C NMR of **2** ($CDCl_3$, 100 MHz).

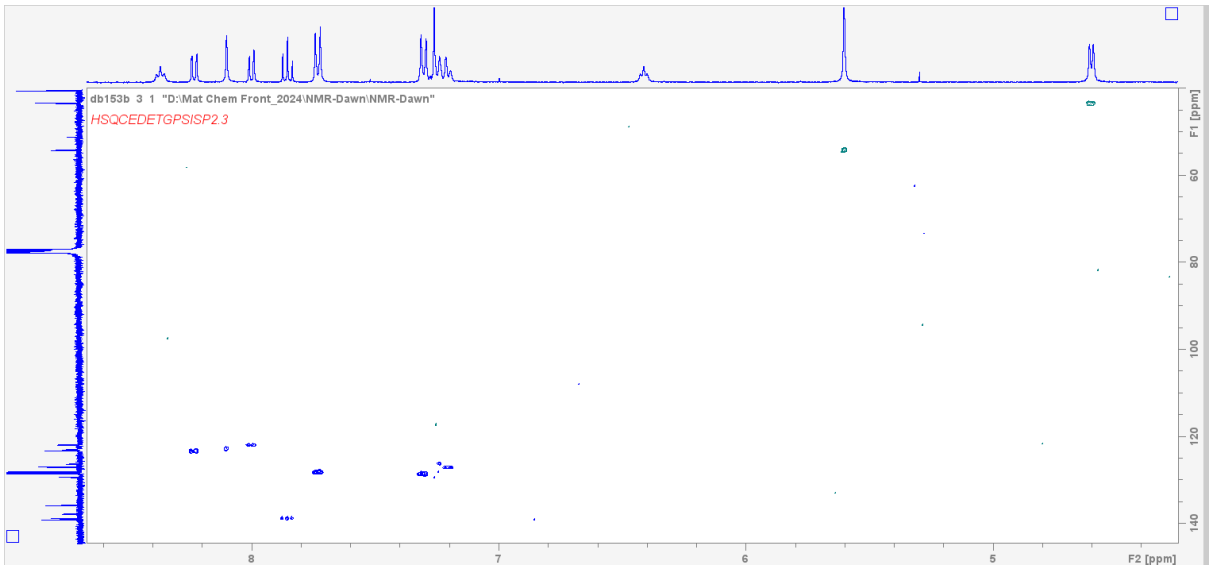

Figure S10. HSQC of **2** ($CDCl_3$)**.**

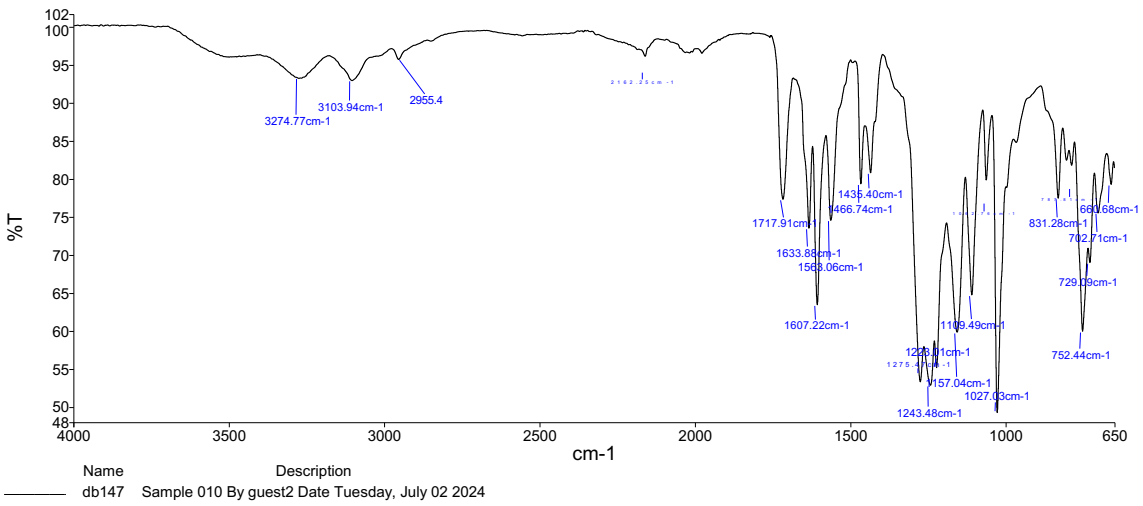

Figure S11. IR of **2**.

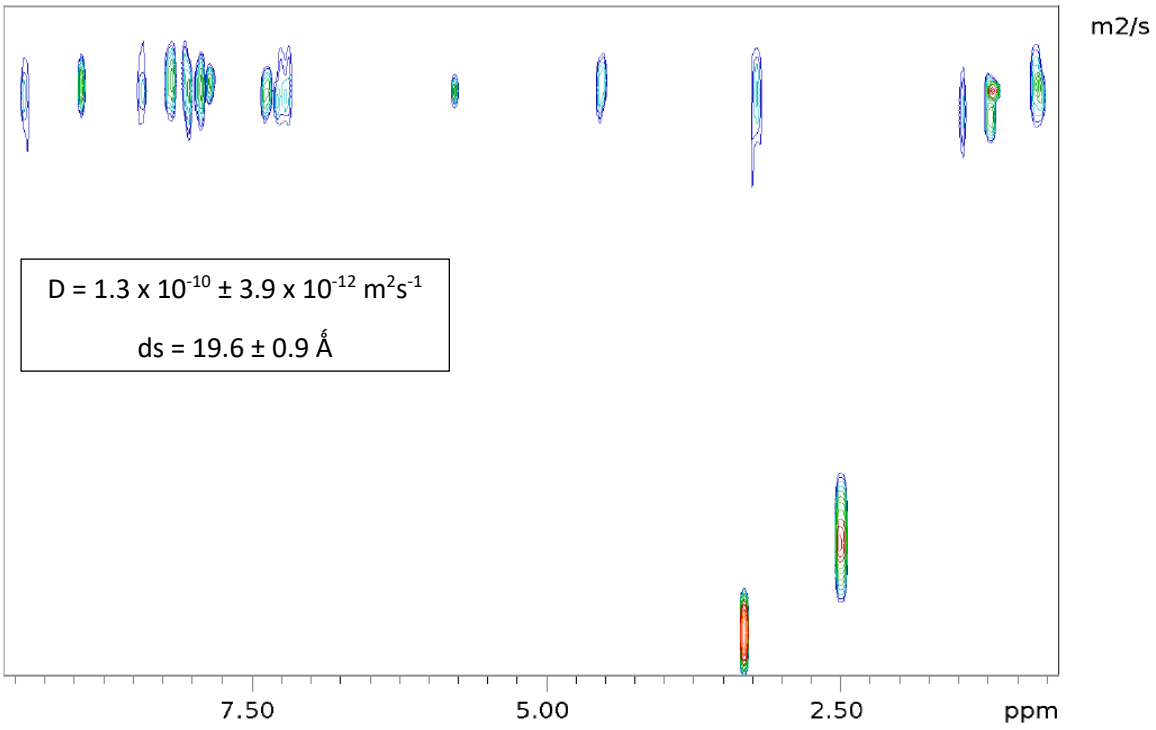

Figure S12. DOSY NMR of **2** (2.0 x 10^{-3} M, DMSO-d_6, 400 MHz).[1]

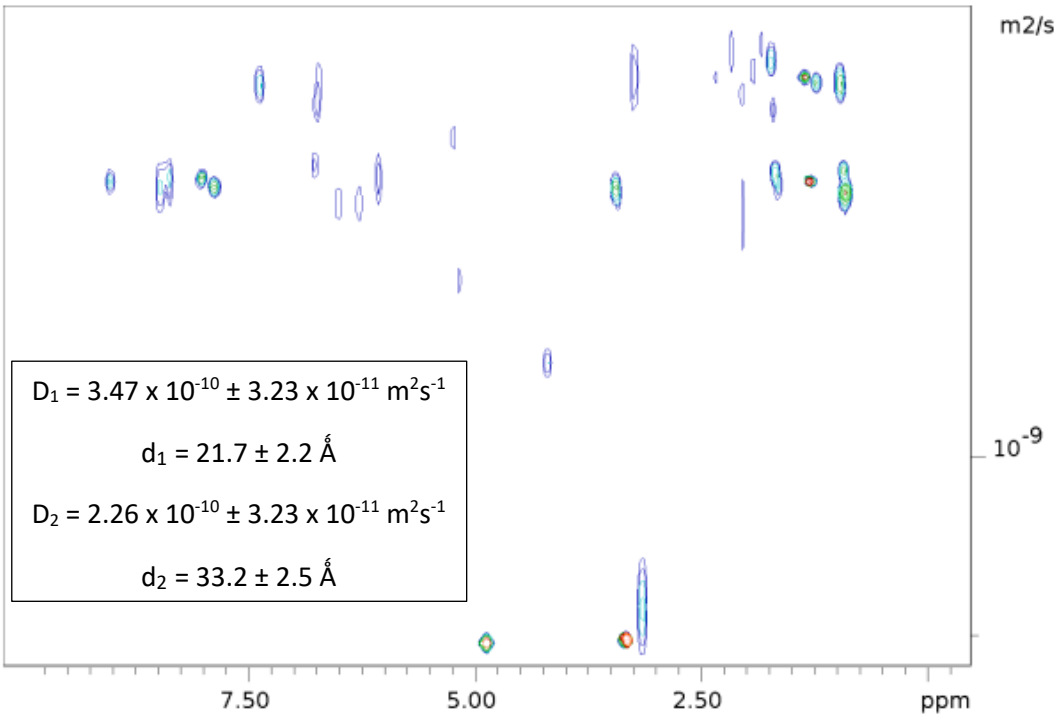

Figure S13: DOSY NMR of **2** (1.7 x 10^{-3} M) with 0.66 equivalents of $Eu(CF_3SO_3)_3$ (CD_3OD, 400 MHz).[2]

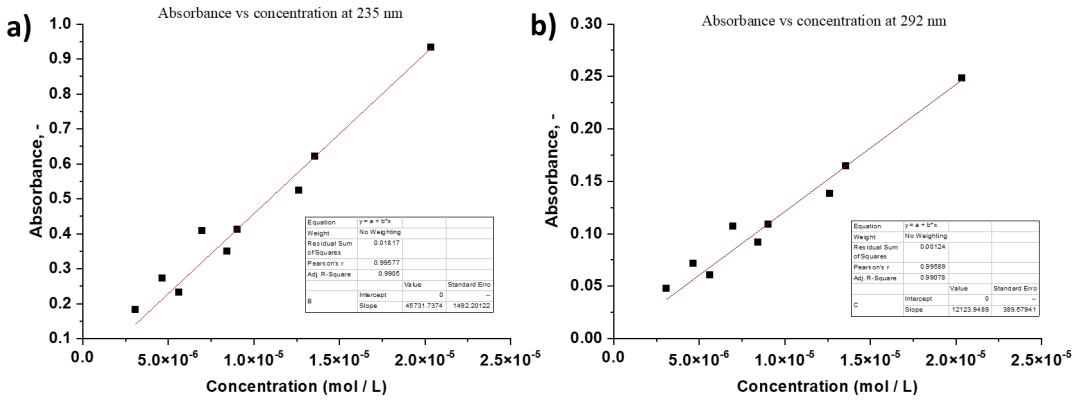

Figure S14. Absorbance of **1** *vs* concentration recorded in CH_3CN at **a)** 235 nm and **b)** 292 nm.

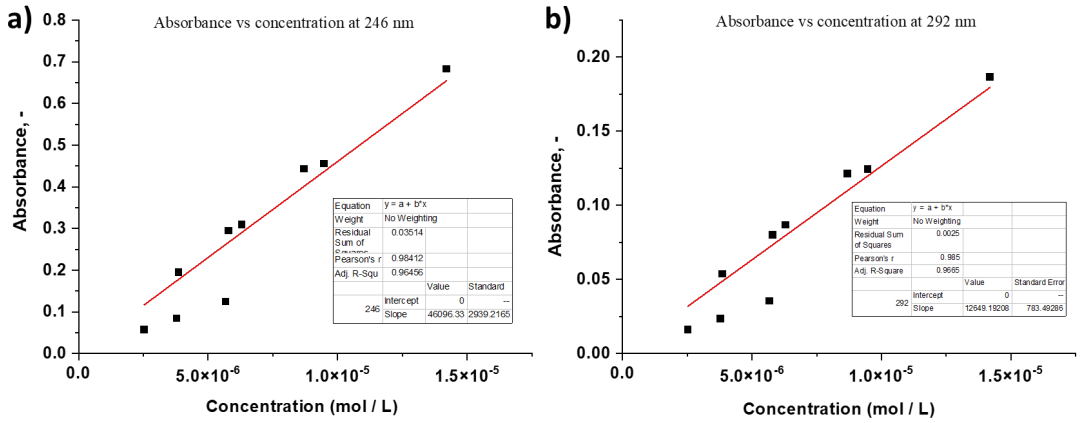

Figure S15. Absorbance of **2** *vs* concentration recorded in CH_3CN:$CHCl_3$ (80:20) at **a)** 235 nm and **b)** 292 nm.

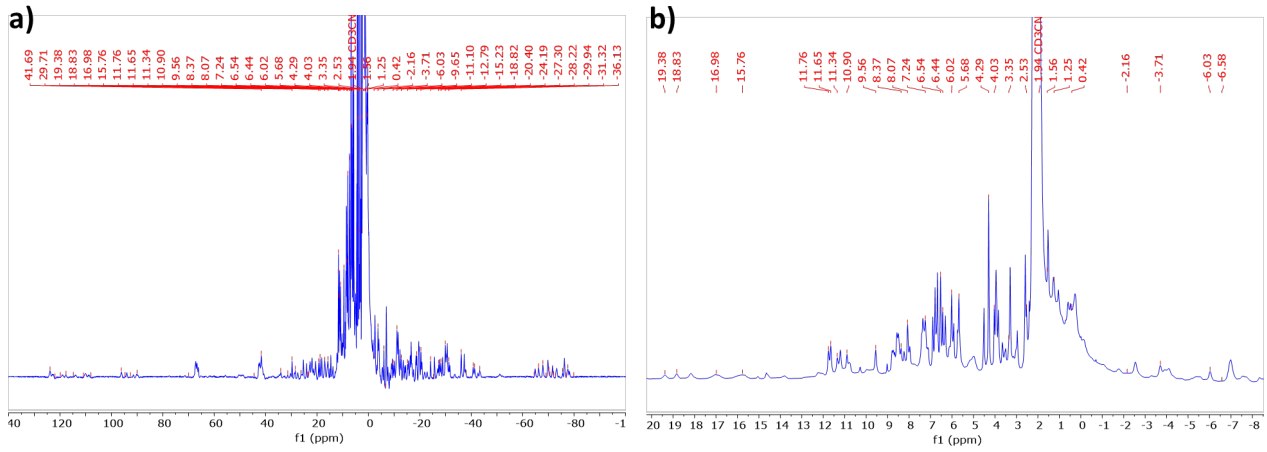

Figure S16. ^{1}H NMR of **3** (400 MHz, CD_3CN): **a)** full spectrum and **b)** zoomed area.

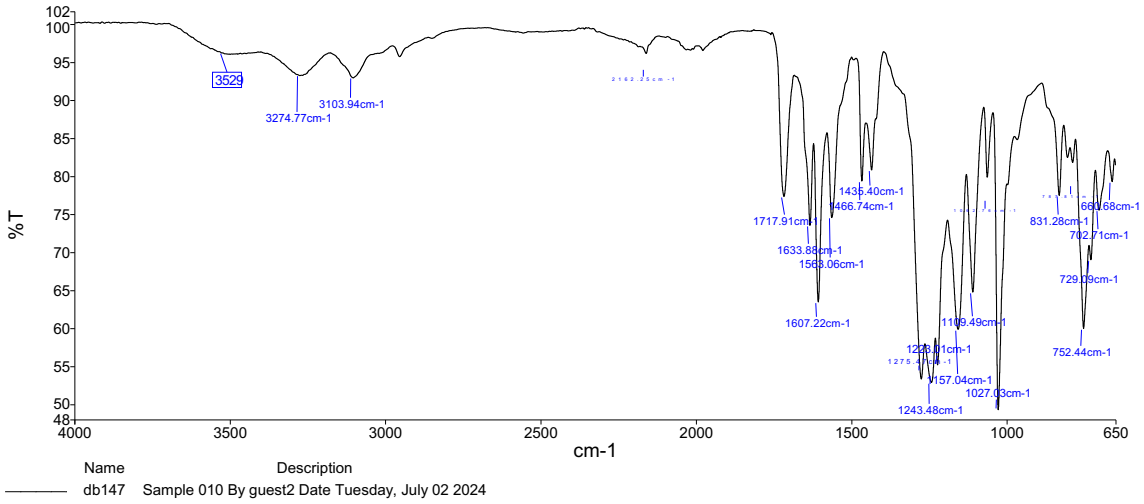

Figure S17. IR of **3**.

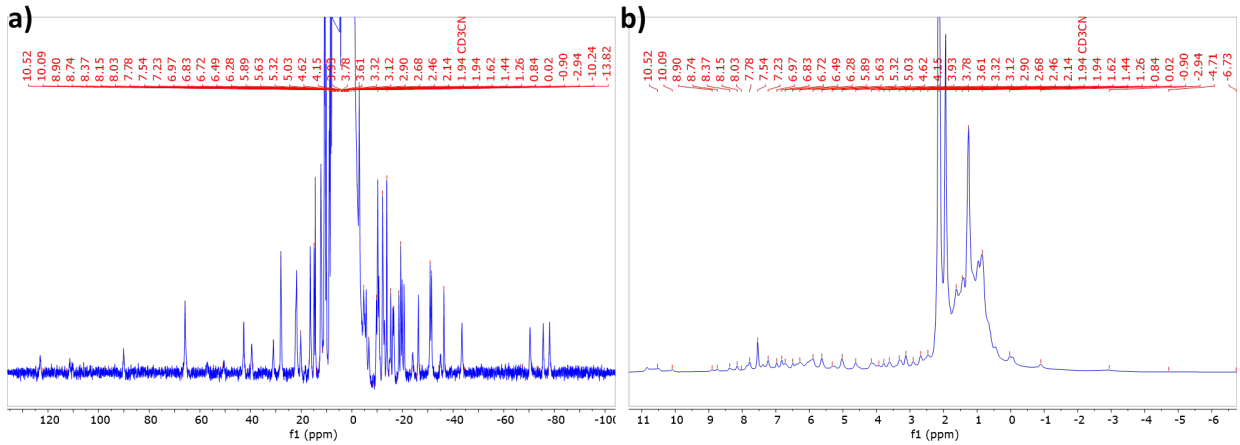

Figure S18. ^{1}H NMR of **4** (400 MHz, CD_3CN): **a)** full spectrum and **b)** zoomed area.

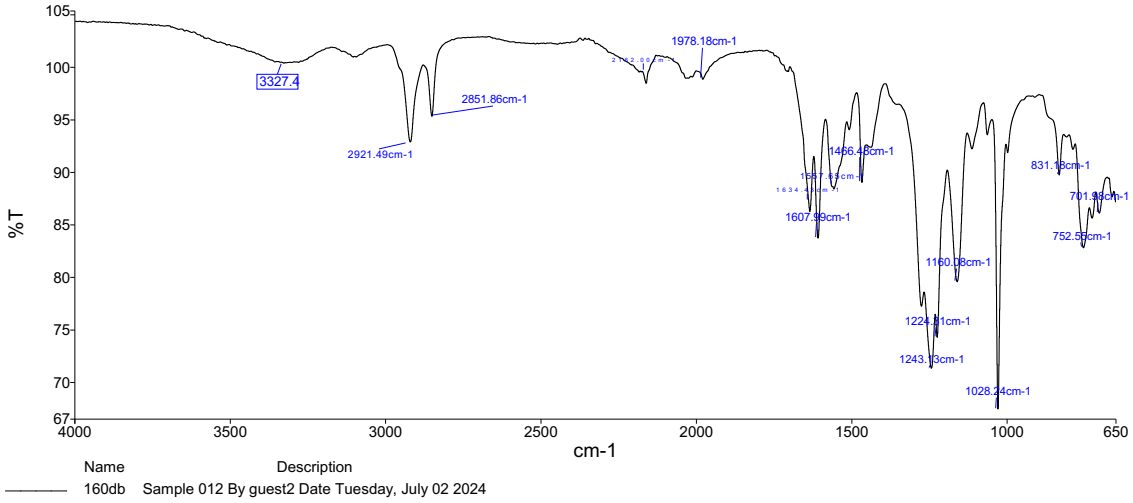

Figure S19. IR of **4**.

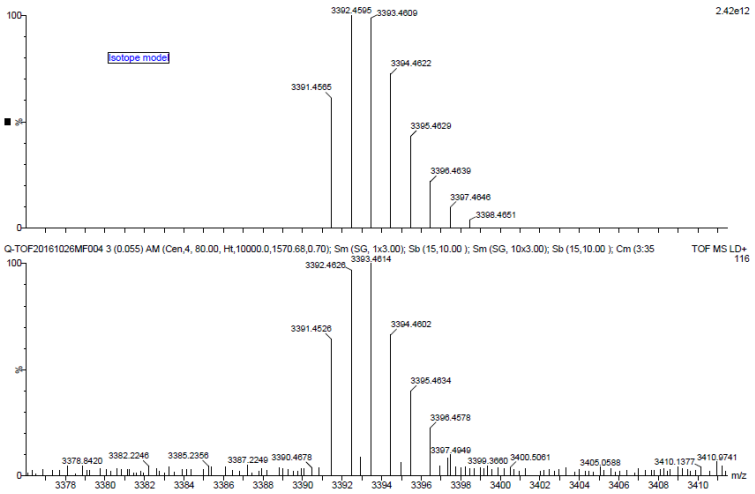

Figure S20. MALDI MS where the experimental and theoretical isotopic distribution are shown for $[\mathbf{Tb_2 1_3}(CF_3SO_3)_5]^+$ ($C_{131}H_{108}F_{15}N_{30}O_{33}S_5Tb_2^+$) of **3**.

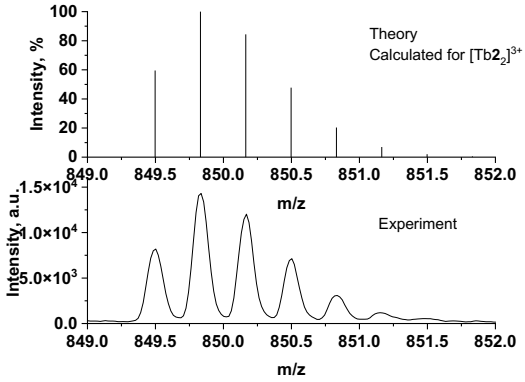

Figure S21. ESI-MS of **4** showing experimental and theoretical isotopic distribution for [Tb**2**$_2$]$^{3+}$.

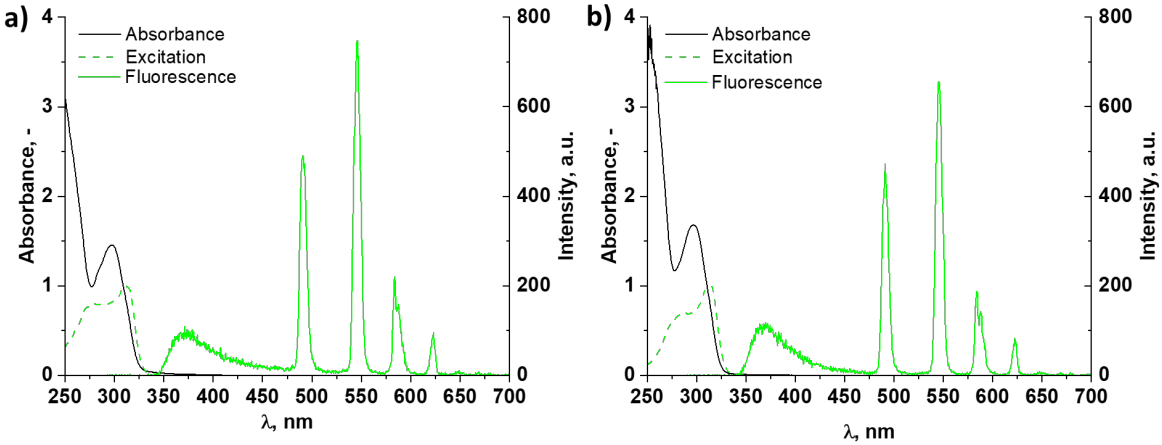

Figure S22. Absorbance, fluorescence (λ_{ex} = 279 nm) and delayed excitation spectra (λ_{em} = 545 nm) of **a) 3** (c = 3.4 × 10^{-4} M) and **b) 4** (c = 2.5 × 10^{-4} M) in CH_3OH.

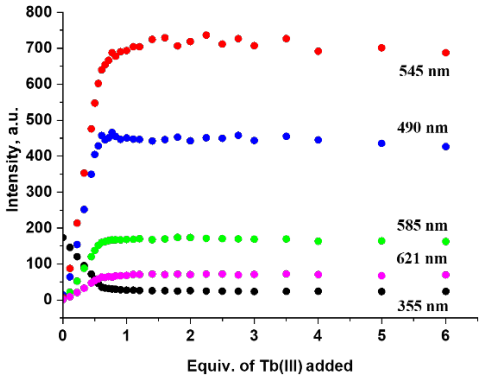

Figure S23. The experimental binding isotherms at λ = 355, 490, 545 and 621 nm of the fluorescence for the titration of **1** (1.0 x 10^{-5} M) against $Tb(CF_3SO_3)_3$ (0 → 6 equiv.) in CH_3CN at 22 °C.

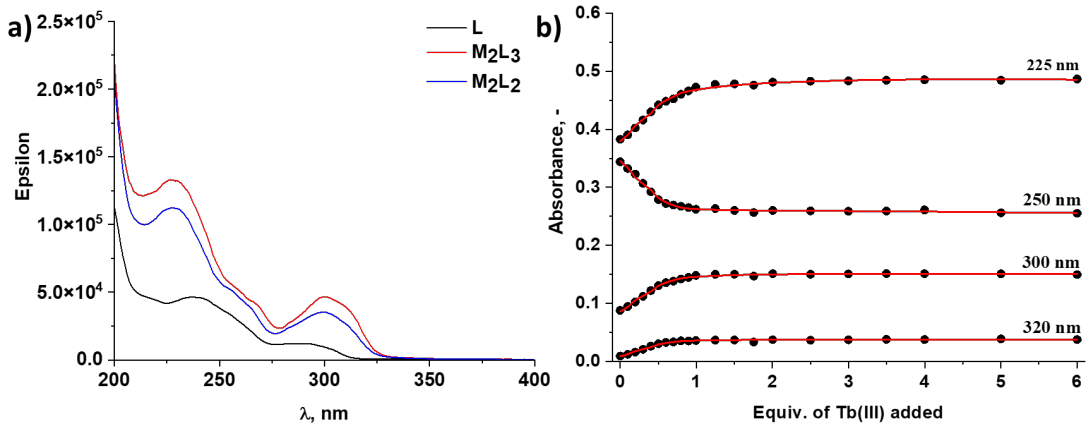

Figure S24. a) Recalculated spectra, **b)** experimental binding isotherms (λ = 225, 250, 300 and 320 nm; •••) and their fit (–) for the titration of **1** (1.0 x 10^{-5} M) against $Tb(CF_3SO_3)_3$ (0 → 6 equiv.) in CH_3CN at 22 °C.

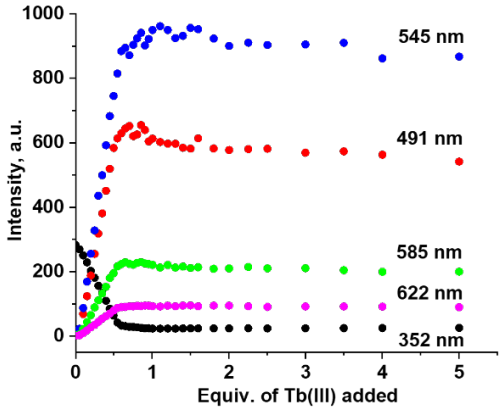

Figure S25. The experimental binding isotherms at λ = 352, 491, 545 and 622 nm of the fluorescence for the titration of **2** (1.1 x 10^{-5} M) against $Tb(CF_3SO_3)_3$ (0 → 6 equiv.) in CH_3CN at 22 °C.

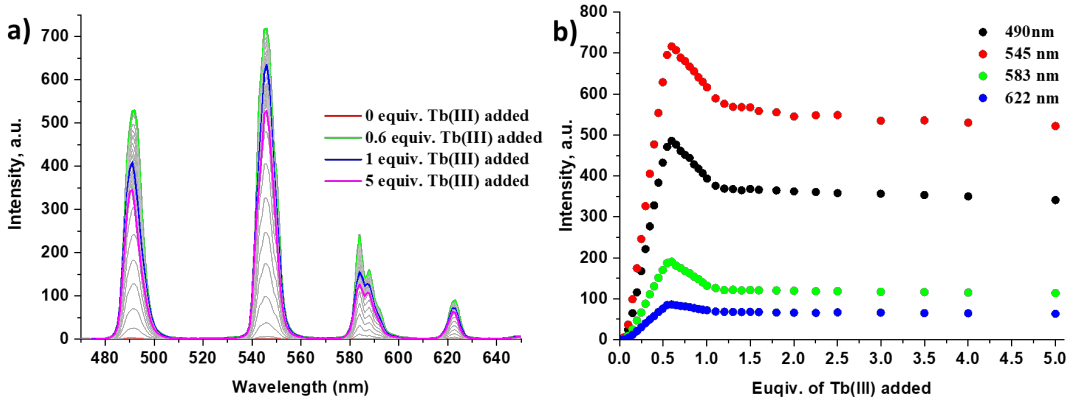

Figure S26. Overall changes in the: **a)** phosphorescence [delayed Tb(III)] emission upon titrating **2** (1.1 x 10^{-5} M) against $Tb(CF_3SO_3)_3$ (0 → 6 equiv.) in CH_3CN at 22 °C (λ_{ex} = 292 nm), and **b)** experimental binding isotherms representing the changes at λ = 490, 545, 583 and 622 nm versus number of equivalents of Tb(III) added to the solution.

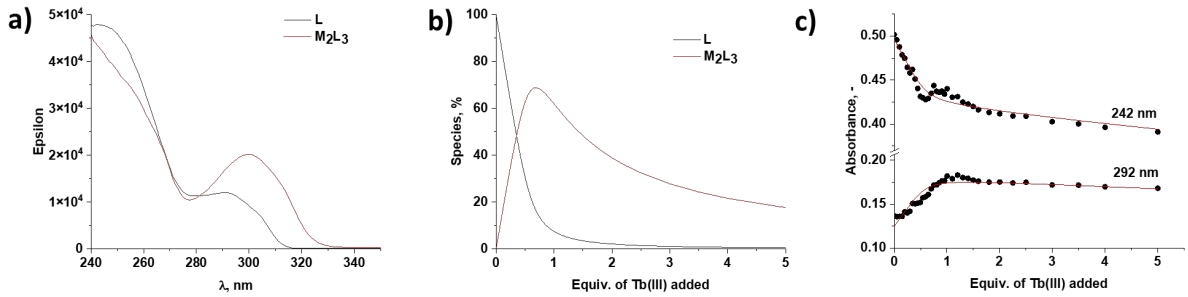

Figure S27. a) Recalculated spectra, **b)** speciation-distribution diagram, **c)** experimental binding isotherms (●●●) and their fit (–) for the titration of **2** (1.1 x 10^{-5} M) against $Tb(CF_3SO_3)_3$ (0 → 6 equiv.) in CH_3CN at 22 °C.

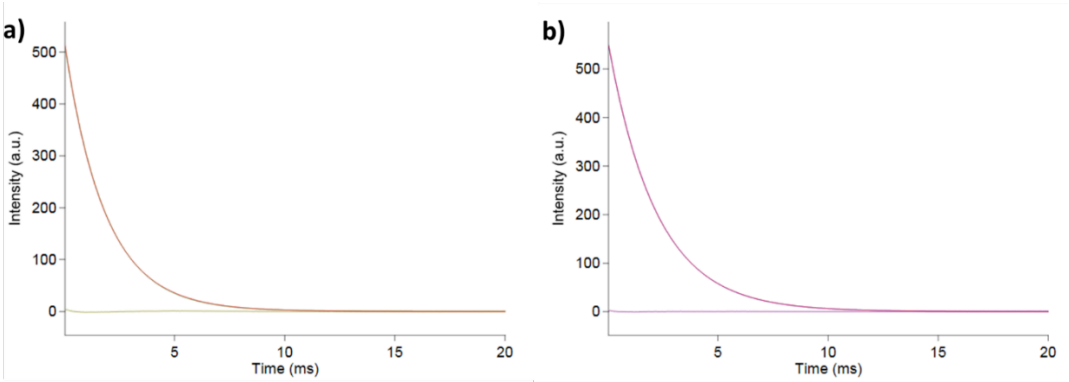

Figure S28. Life-times of Tb(III)-centred emission (λ_{ex} = 292 nm; λ_{em} = 545 nm) decays and their mono-exponential fits recorded for **3** in **a)** CH_3OH and **b)** CD_3OD.

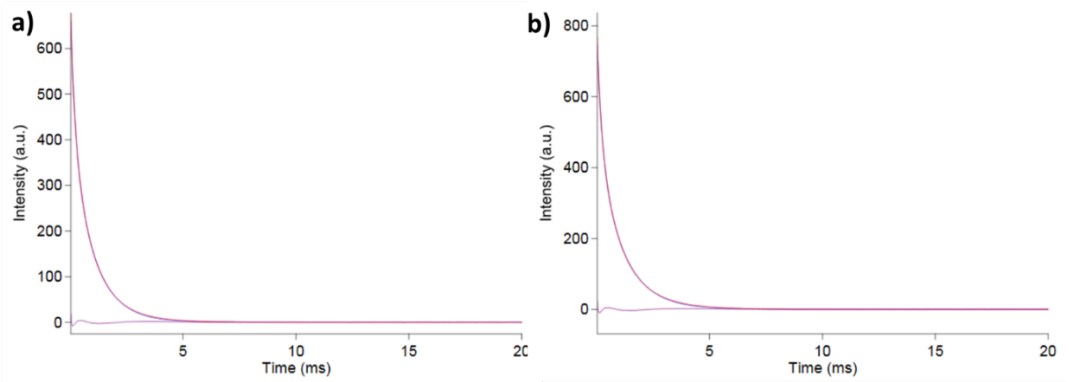

Figurer S29. Life-times of Tb(III)-centred emission (λ_{ex} = 292 nm; λ_{em} = 545 nm) decays and their bi-exponential fits recorded for **3** in **a)** H_2O and **b)** D_2O.

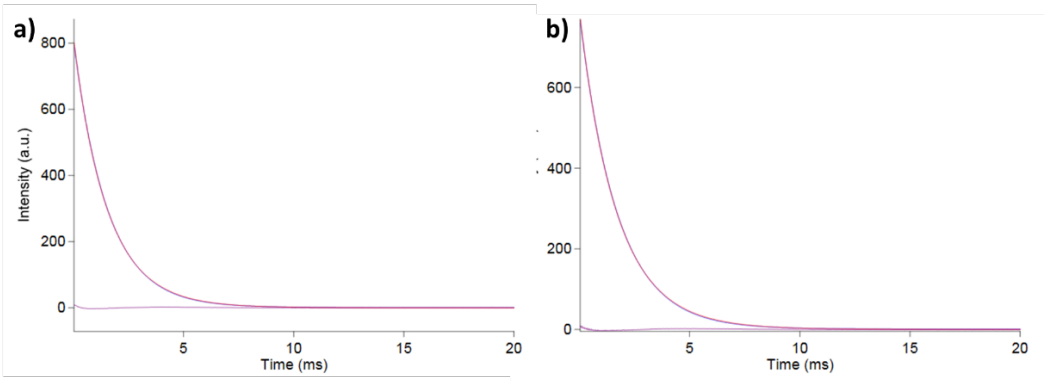

Figure S30. Life-times of Tb(III)-centred emission (λ_{ex} = 292 nm; λ_{em} = 545 nm) decays and their mono-exponential fits recorded for **4** in **a)** CH_3OH and **b)** CD_3OD.

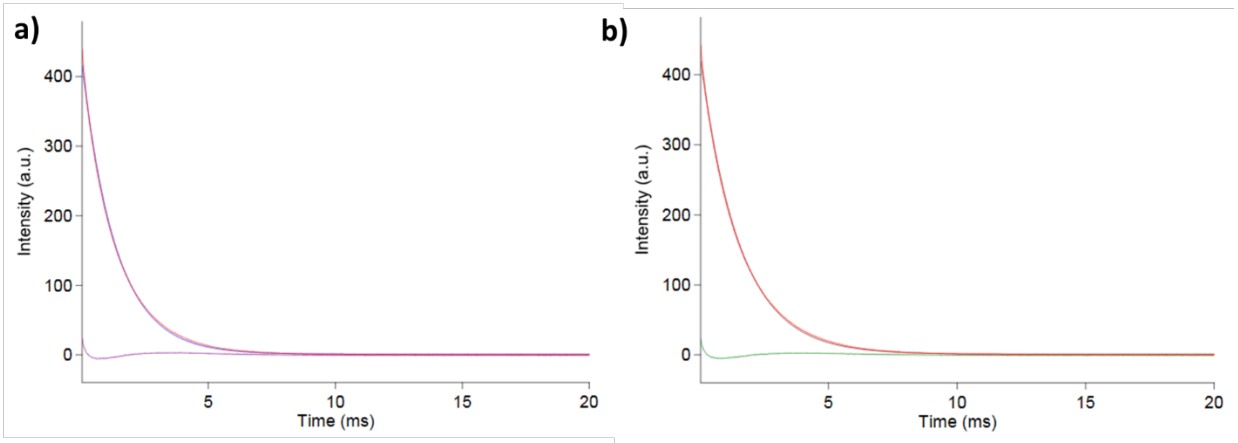

Figurer S31. Life-times of Tb(III)-centred emission (λ_{ex} = 292 nm; λ_{em} = 545 nm) decays and their mono-exponential fits recorded for **4** in **a)** H_2O and **b)** D_2O.

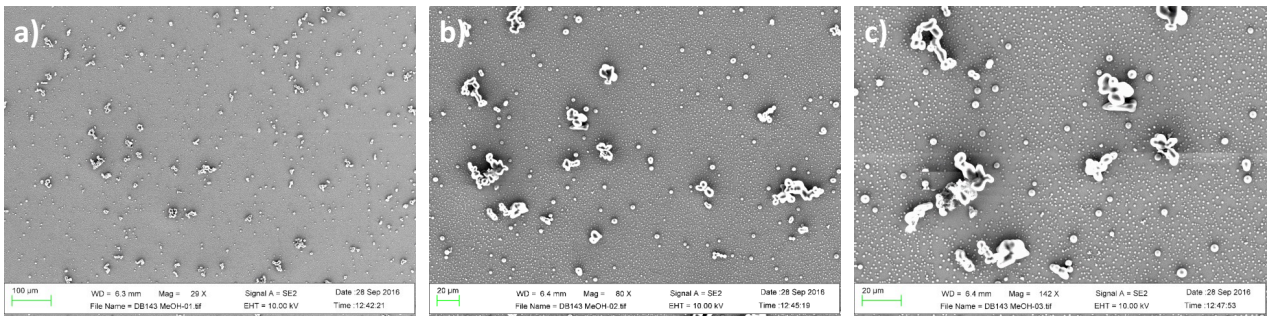

Figure S32. SEM Images of sample **1** prepared in MeOH [0.5 % w/v (2 mg in 400 µL)] where 10 µL of solution was deposited onto silica wafers and dried overnight: **a)** [scale bar = 100 µm], **b)** [scale bar = 20 µm], and **c)** [scale bar = 20 µm], respectively.

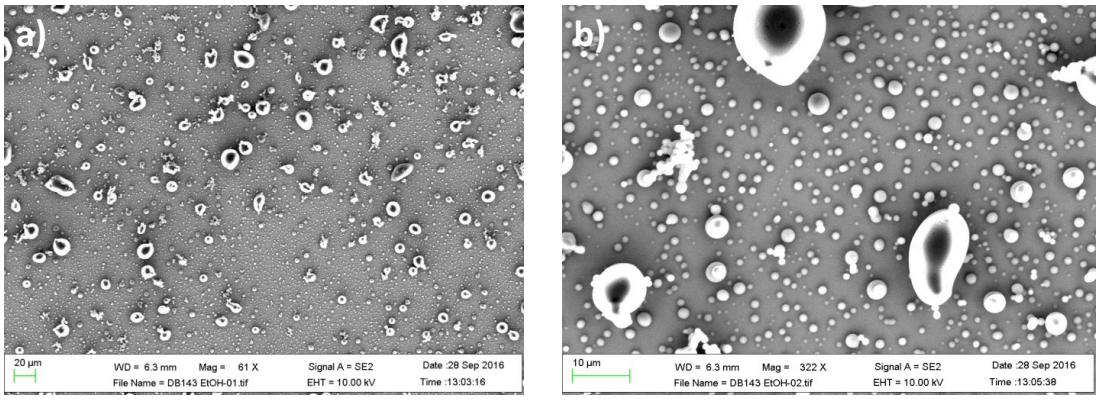

Figure S33. SEM Images of sample **1** prepared in EtOH [0.5 % w/v (2 mg in 400 µL)] where 10 µL of solution was deposited onto silica wafers and dried overnight: **a)** [scale bar = 20 µm],and **b)** [scale bar = 10 µm], respectively.

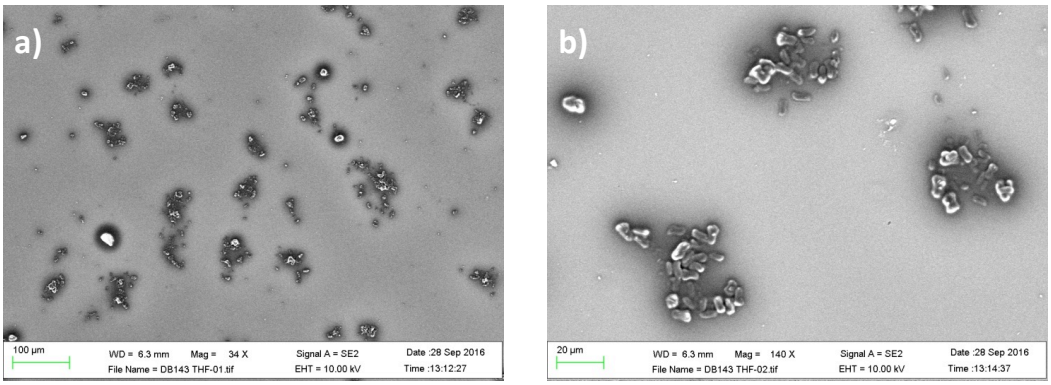

Figure S34. SEM Images of sample **1** prepared in THF [0.5 % w/v (2 mg in 400 µL)] where 10 µL of solution was deposited onto silica wafers and dried overnight: **a)** [scale bar = 100 µm], and **b)** [scale bar = 20 µm], respectively.

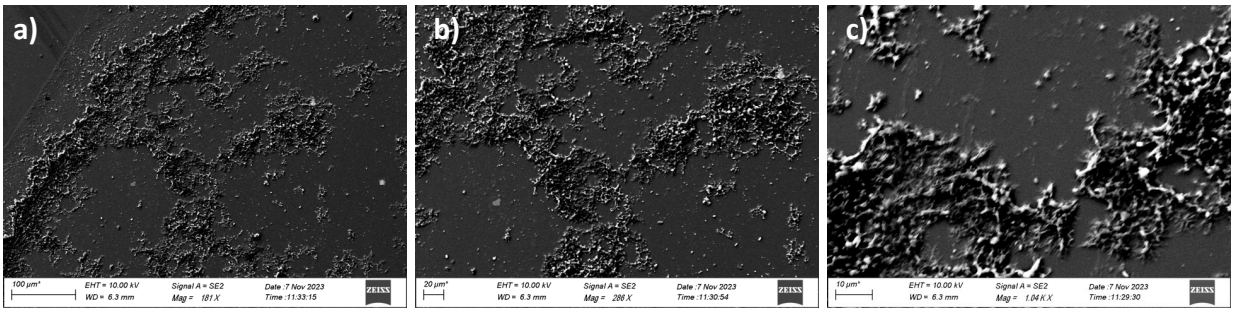

Figure S35. SEM Images of samples **2** prepared in MeOH [0.5 % w/v (2 mg in 400 µL)] where 10 µL of solution was deposited onto silica wafers and dried overnight: **a)** [scale bar = 100 µm], **b)** [scale bar = 20 µm], and **c)** [scale bar = 10 µm], respectively.

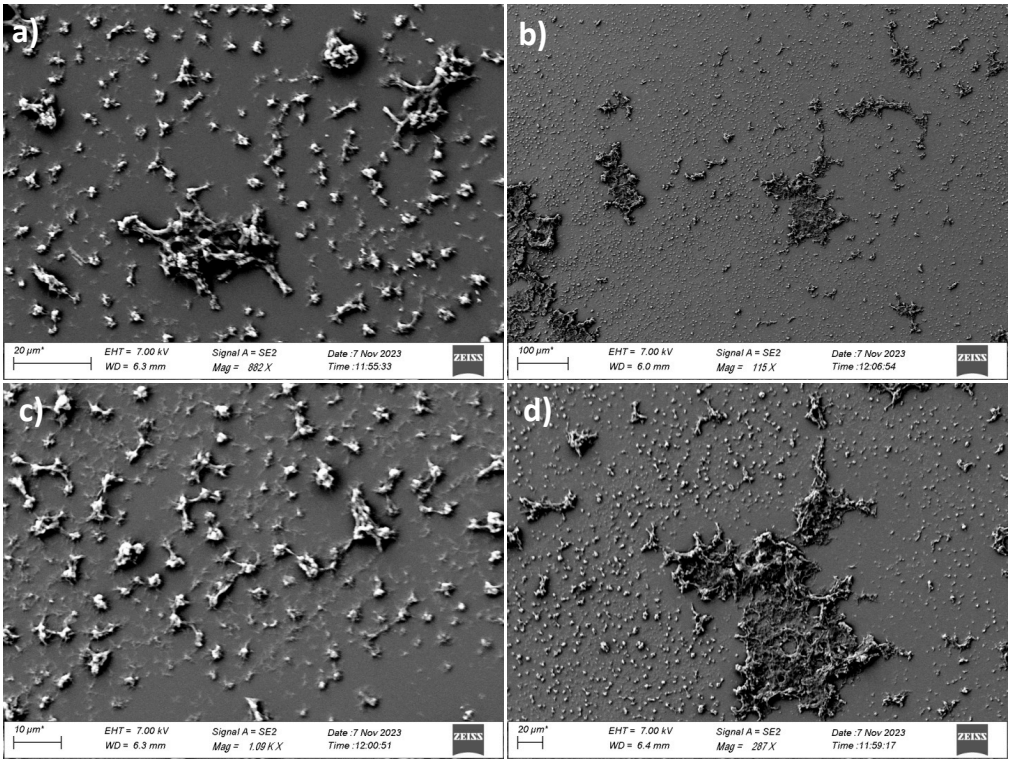

Figure S36. SEM Images of samples **2** prepared in EtOH [0.5 % w/v (2 mg in 400 µL)] where 10 µL of solution was deposited onto silica wafers and dried overnight: **a)** [scale bar = 20 µm], **b)** [scale bar = 100 µm], **c)** [scale bar = 10 µm], **d)** [scale bar = 20 µm], respectively.

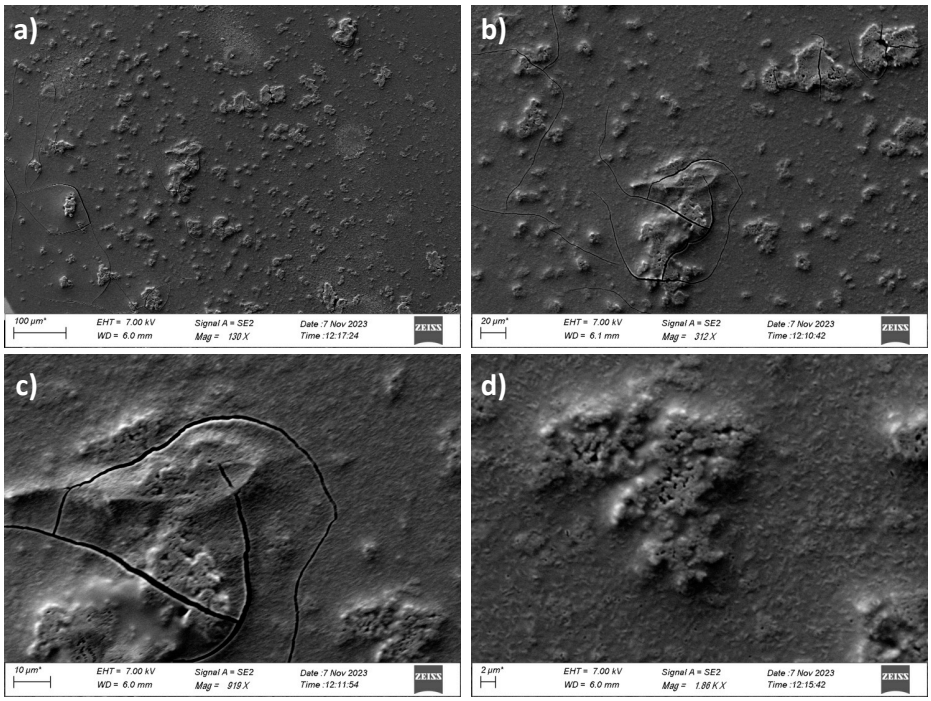

Figure S37. SEM Images of samples **2** prepared in THF [0.5 % w/v (2 mg in 400 µL)] where 10 µL of solution was deposited onto silica wafers and dried overnight: **a)** [scale bar = 100 µm], **b)** [scale bar = 20 µm], **c)** [scale bar = 10 µm], and **d)** [scale bar = 20 µm], respectively.

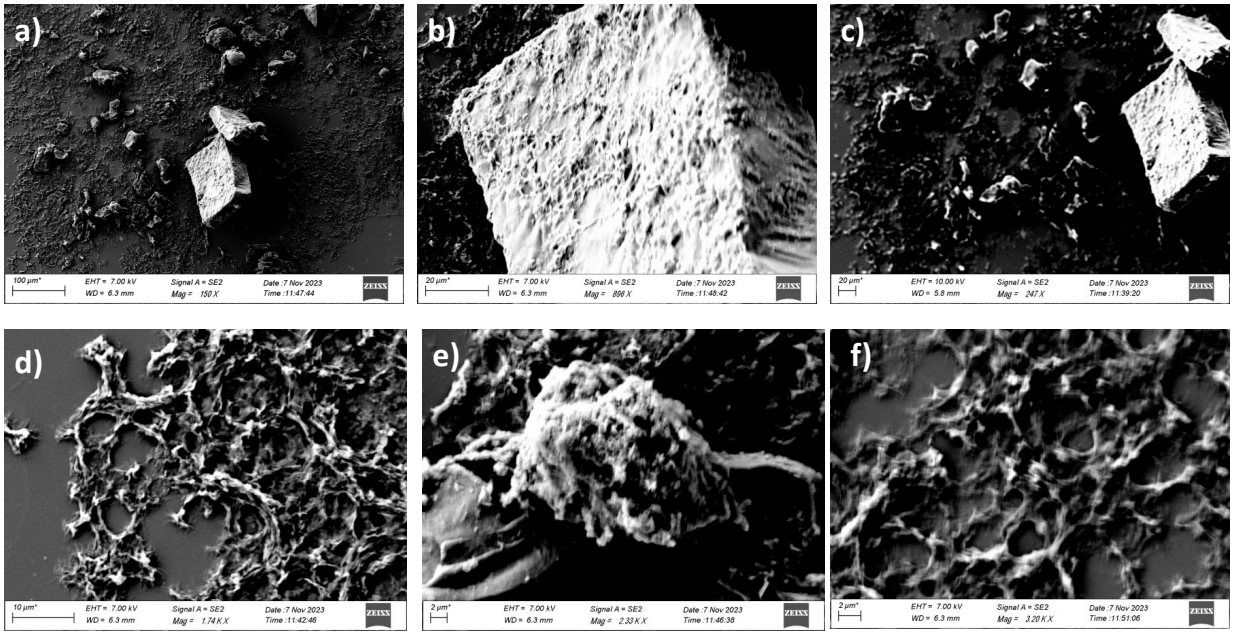

Figure S38. SEM Images of samples **2** prepared in MeOH [1.0 % w/v (2 mg in 200 µL)] where 10 µL of solution was deposited onto silica wafers and dried overnight: **a)** [scale bar = 100 µm], **b)** [scale bar = 20 µm], **c)** [scale bar = 20 µm], **d)** [scale bar = 10 µm], **e)** [scale bar = 2 µm], and **f)** [scale bar = 2 µm], respectively.

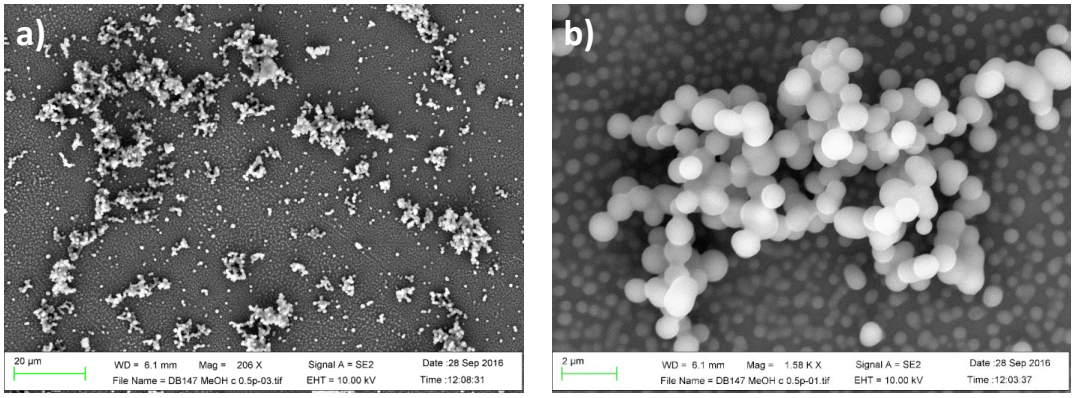

Figure S39. SEM Images of samples **3** prepared in MeOH [0.5 % w/v (2 mg in 400 µL)] where 10 µL of solution was deposited onto silica wafers and dried overnight: **a)** [scale bar = 20 µm], and **b)** [scale bar = 2 µm], respectively.

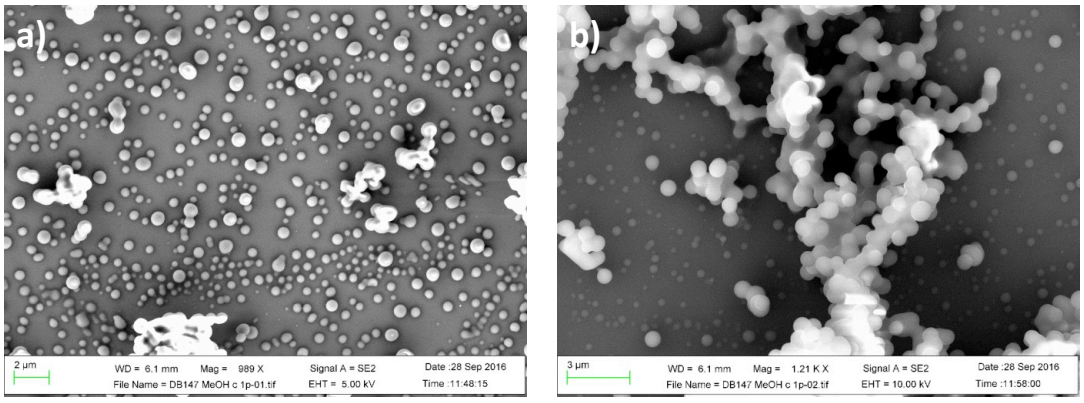

Figure S40. SEM Images of samples **3** prepared in MeOH [1.0 % w/v (2 mg in 200 µL)] where 10 µL of solution was deposited onto silica wafers and dried overnight: **a)** [scale bar = 2 µm], and **b)** [scale bar = 3 µm], respectively.

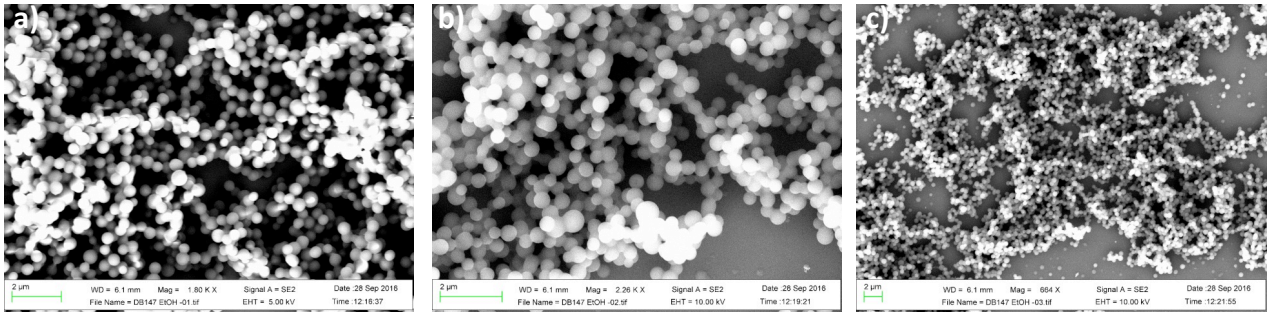

Figure S41. SEM Images of samples **3** prepared in EtOH [0.5 % w/v (2 mg in 400 µL)] where 10 µL of solution was deposited onto silica wafers and dried overnight: **a)** [scale bar = 2 µm], **b)** [scale bar = 2 µm], and **c)** [scale bar = 2 µm], respectively.

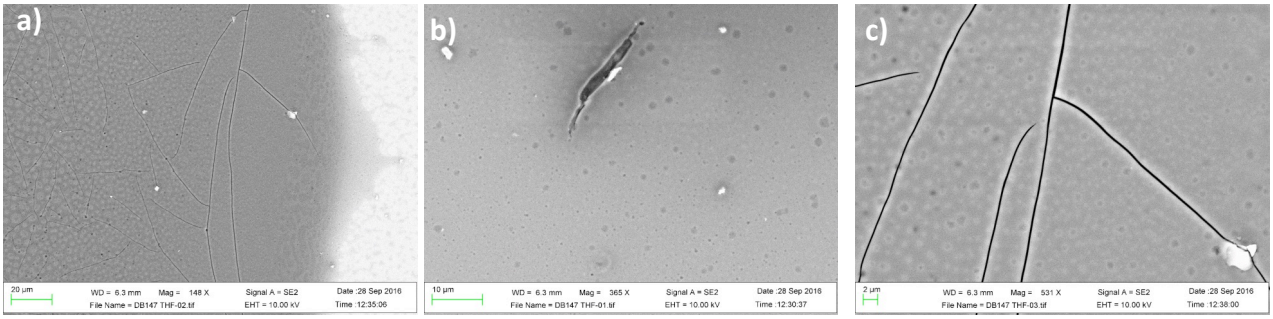

Figure S42. SEM Images of samples **3** prepared in THF [0.5 % w/v (2 mg in 400 µL)] where 10 µL of solution was deposited onto silica wafers and dried overnight: **a)** [scale bar = 20 µm], **b)** [scale bar = 10 µm], and **c)** [scale bar = 2 µm], respectively.

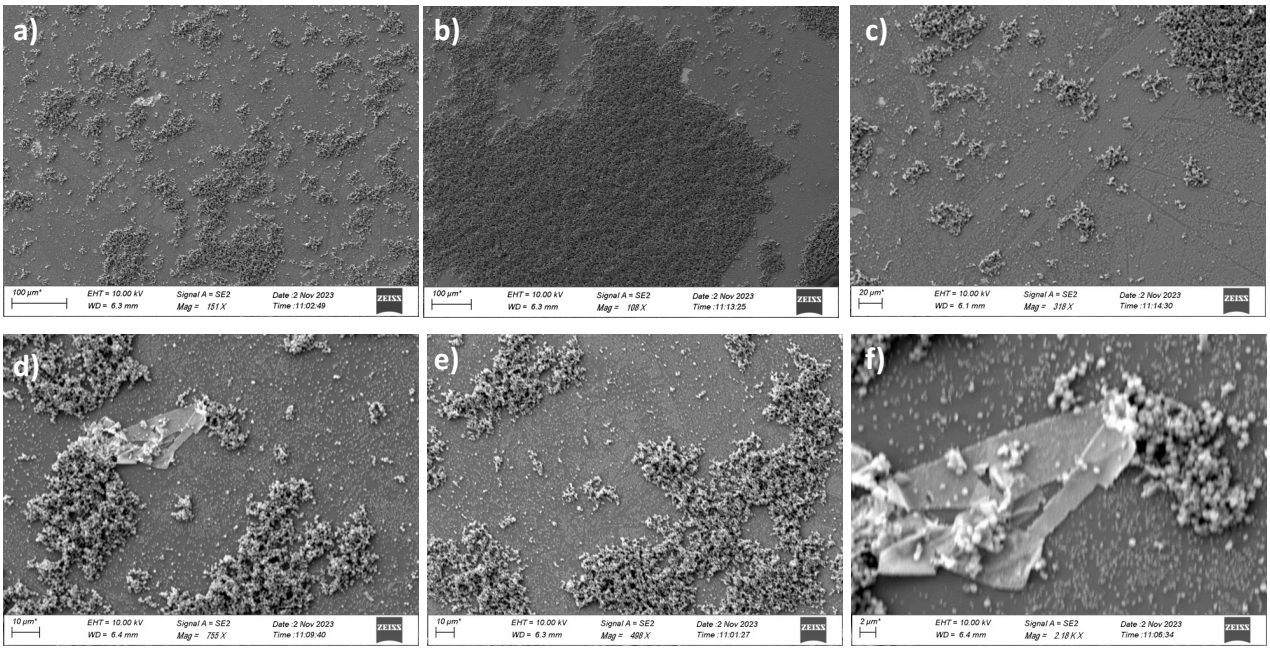

Figure S43. SEM Images of samples **4** prepared in MeOH [1.0 % w/v (2 mg in 200 µL)] where 10 µL of solution was deposited onto silica wafers and dried overnight: **a)** [scale bar = 100 µm], **b)** [scale bar =

100 µm], **c)** [scale bar = 20 µm], **d)** [scale bar = 10 µm], and **e)** [scale bar = 10 µm], and **f)** [scale bar = 2 µm], respectively.

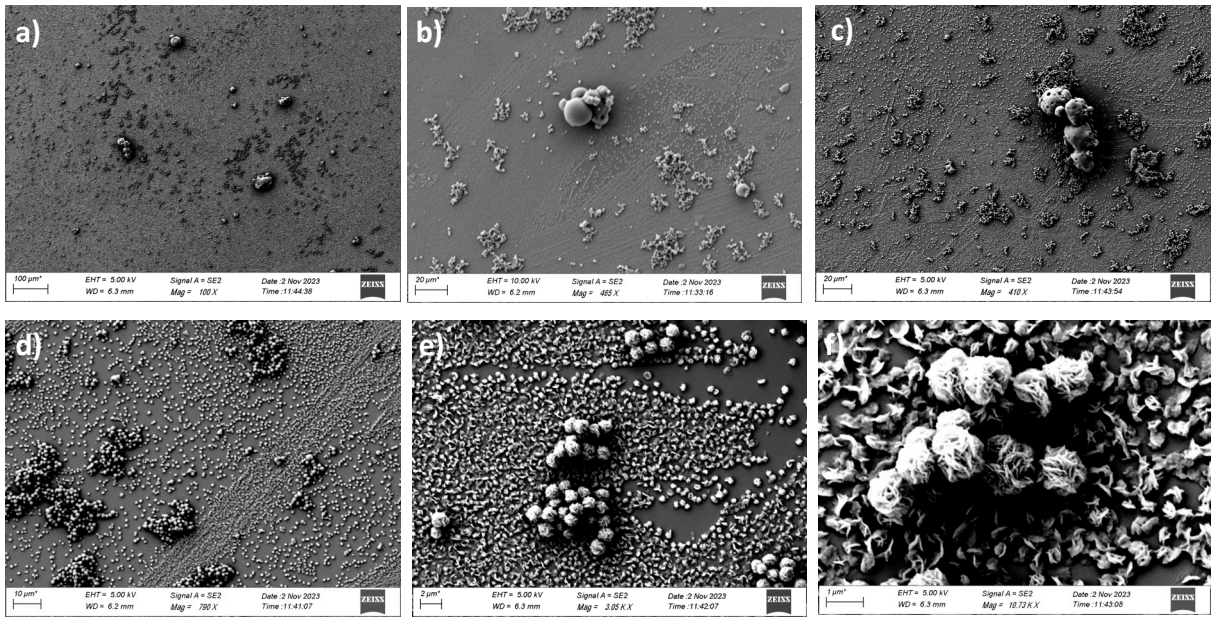

Figure S44. SEM Images of samples **4** prepared in EtOH [0.5 % w/v (2 mg in 400 µL)] where 10 µL of solution was deposited onto silica wafers and dried overnight: **a)** [scale bar = 100 µm], **b)** [scale bar = 20 µm], **c)** [scale bar = 20 µm], **d)** [scale bar = 10 µm], and **e)** [scale bar = 2 µm], and **f)** [scale bar = 1 µm], respectively.

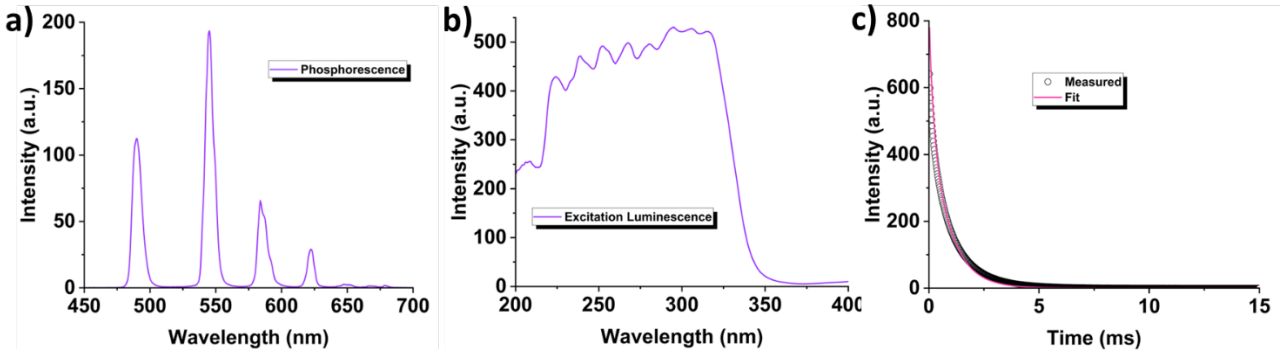

Figurer S45. a) The emission (λ_{ex} = 290 nm) and **b)** excitation (λ_{em} = 545 nm) spectra recorded for the solid **3** in phosphorescence mode. **c)** The excited state decay recorded in phosphorescence mode (λ_{em} = 545 nm), which was best fitted to bi-exponential decay (λ_{ex} = 290 nm).

References

1. H. Günther, NMR spectroscopy: Basic principles, concepts, and applications in chemistry, Wiley-VCH, 2013.